"Advanced desalination of dye/NaCl mixtures by a loose nanofiltration membrane for digital ink-jet printing"

Ye, Wenyuan ; Lin, Jiuyang ; Borrego, Ricard ; Chen, Dong ; Sotto, Arcadio ; Luis Alconero, Patricia ; Liu, Minghua ; Zhao, Shuaifei ; Tang, Chuyang Y. ; Van der Bruggen, Bart

ABSTRACT

In digital printing, a high salt content in dye solutions is detrimental, which calls for effective strategy for dye/salt fractionation. In this study, a loose nanofiltration (NF) membrane Sepro 2A was employed to desalinate diverse dye species (2 reactive dyes and 4 cationic dyes). This membrane, with a molecular weight cutoff of 490 Da, showed consistently high rejections to all the reactive and cationic dyes (>97.7%). Operational conditions such as dye concentrations and applied pressures have limited effects on the rejection of the membrane. An integrated NF-diafiltration process, involving a pre-concentration and a diafiltration step, was specifically designed for the fractionation of dye/NaCl mixtures. This loose NF membrane showed >99.7% rejection to reactive dyes (reactive blue 2 and reactive orange 16) and ca. 99.3% salt removal with ca. 2.0% dye loss after 5.0 diavolumes. However, the NF membrane experienced a 15.9% loss to methylene blue due to the lower rejection to this model cationic dye (97.2%). The current study provides important insights into dye/salt fractionation by loose NF membranes for digital ink-jet printing. © 2017 Elsevier B.V.

CITE THIS VERSION

Ye, Wenyuan ; Lin, Jiuyang ; Borrego, Ricard ; Chen, Dong ; Sotto, Arcadio ; et. al. *Advanced desalination of dye/NaCl mixtures by a loose nanofiltration membrane for digital ink-jet printing.* In: *Separation and Purification Technology*, Vol. 197, no. 1, p. 27-35 (2018) http://hdl.handle.net/2078.1/217563 -- DOI : 10.1016/j.seppur.2017.12.045

Separation and Purification Technology 197 (2018) 27–35

Contents lists available at ScienceDirect

Separation and Purification Technology

journal homepage: www.elsevier.com/locate/seppur

Advanced desalination of dye/NaCl mixtures by a loose nanofiltration membrane for digital ink-jet printing

Wenyuan Ye[a], Jiuyang Lin[b,*], Ricard Borrego[c], Dong Chen[d], Arcadio Sotto[e], Patricia Luis[f], Minghua Liu[b,*], Shuaifei Zhao[g], Chuyang Y. Tang[h], Bart Van der Bruggen[i]

[a] *Fujian Provincial Key Laboratory of Soil Environmental Health and Regulation, College of Resources and Environment, Fujian Agriculture and Forestry University, Fuzhou 350002, China*
[b] *School of Environment and Resources, Qi Shan Campus, Fuzhou University, No. 2 Xueyuan Road, University Town, 350116 Fuzhou, Fujian, China*
[c] *Department of Chemical Engineering, Universitat Rovira i Virgili, 43207 Tarragona, Spain*
[d] *Department of Urology, Sun Yat-Sen University Cancer Center, 510060 Guangzhou, China*
[e] *Department of Chemical and Environmental Technology, Rey Juan Carlos University, 28933 Móstoles, Madrid, Spain*
[f] *Materials & Process Engineering (iMMC-IMAP), Université catholique de Louvain, 1348 Louvain-la-Neuve, Belgium*
[g] *Department of Environmental Sciences, Faculty of Science and Engineering, Macquarie University, Sydney, NSW 2109, Australia*
[h] *Department of Civil Engineering, The University of Hong Kong, Pokfulam HW619B, Hong Kong*
[i] *Department of Chemical Engineering, Process Engineering for Sustainable Systems (ProcESS), KU Leuven, Celestijnenlaan 200F, B-3001 Leuven, Belgium*

A R T I C L E I N F O

Keywords:
Loose nanofiltration membrane
Fractionation
Dye/salt mixture
Diafiltration
Digital printing

A B S T R A C T

In digital printing, a high salt content in dye solutions is detrimental, which calls for effective strategy for dye/salt fractionation. In this study, a loose nanofiltration (NF) membrane Sepro 2A was employed to desalinate diverse dye species (2 reactive dyes and 4 cationic dyes). This membrane, with a molecular weight cutoff of 490 Da, showed consistently high rejections to all the reactive and cationic dyes (>97.7%). Operational conditions such as dye concentrations and applied pressures have limited effects on the rejection of the membrane. An integrated NF-diafiltration process, involving a pre-concentration and a diafiltration step, was specifically designed for the fractionation of dye/NaCl mixtures. This loose NF membrane showed >99.7% rejection to reactive dyes (reactive blue 2 and reactive orange 16) and ca. 99.3% salt removal with ca. 2.0% dye loss after 5.0 diavolumes. However, the NF membrane experienced a 15.9% loss to methylene blue due to the lower rejection to this model cationic dye (97.2%). The current study provides important insights into dye/salt fractionation by loose NF membranes for digital ink-jet printing.

1. Introduction

Digital ink-jet printing, based on the CMYK (i.e., cyan, magenta, yellow and black) color models, is widely used to print computer image files due to its short process run, fast response time, environmental safety and mass customization in the textile industry [1]. Generally, the ink-jet dyes are highly concentrated colorants which require high purity and very low salt content to ensure high quality printing. However, the dyes are mainly produced by chemical synthesis along with the generation of byproduct salts (ca. 5.0 wt% NaCl) as impurity, substantially diminishing the purity of dye products [2]. Specifically, the high salt content compromises the stability of the ink-jet dyes, reducing the image brilliance, but also induces clogging in the nozzle and corrosion during digital printing [1]. Therefore, advanced purification technologies are urgently required for improving the purity of ink-jet dyes.

Nanofiltration (NF) has become an attractive option for the fractionation of organic matter and salt mixtures [3], including dye/salt fractionation with a high selectivity for dye molecules and partial passage for monovalent inorganic salts [4–6]. Several commercial NF membranes, such as DS5 DK (GE Osmonics) [7], TFC-SR2 (Koch) [8], and NF 90 (Dow Film-Tech) [9], show nearly complete dye rejection. However, these membranes with dense surface morphology usually have a low salt permeation, leading to low efficiency for fractionation of dye/salt mixtures and reduced water permeation at high osmotic pressure difference [10]. For example, Koyuncu et al. reported ca. 75% permeate flux loss of DS5 DK membrane when the NaCl concentration in the reactive black 5/NaCl binary mixture increased from $0\,g\,L^{-1}$ to $80\,g\cdot L^{-1}$ at an applied pressure of 8 bar [11].

Loose NF membranes can be an alternative to conventional dense NF membranes to enhance the fractionation of dye/salt mixtures. Their

* Corresponding authors.
E-mail addresses: jiuyang.lin@fzu.edu.cn, linjiuyang@126.com (J. Lin), mhliu2000@fzu.edu.cn (M. Liu).

https://doi.org/10.1016/j.seppur.2017.12.045
Received 5 November 2017; Received in revised form 7 December 2017; Accepted 27 December 2017
Available online 27 December 2017

larger pore size facilitates efficient salt permeation while sustaining high retention to dye molecules, resulting in an improved selectivity of dyes over salts [12–14]. Our previous study demonstrated great potential of loose NF membranes for dye recovery from textile wastewater, since a very high rejection to direct dyes (>99.6% for Congo red, direct red 23 and direct red 80) and high NaCl transmission (ca. 95.4%) were achieved [4]. A novel loose NF membrane functionalized with copper nanoparticles via bio-inspired deposition offered rejection coefficient of >99.5% to dyes (i.e., Congo red, direct red 23 and reactive blue 2) and 96.3% NaCl permeation [12]. It is worthwhile to note that earlier studies largely focused on the application of (tight) nanofiltration membranes for dye removal from textile wastewater for water recovery [15–18]. Systematic studies on the use of commercial loose NF membranes for purification of reactive dyes and cationic dyes for digital printing are still limited. In particular, the relationship between solute (dyes) structures and the performance of loose NF membrane has not been well documented yet.

In this study, a loose NF membrane (Sepro NF 2A) was employed to purify various dyes (i.e., 2 reactive and 4 cationic dyes) for digital inkjet printing. The solute structure-membrane performance relation was systematically explored. Specifically, the filtration behaviors of the loose NF membrane in single- (pure dye solutions) or multi-component (dye/NaCl binary mixtures) solutions were determined at variable operating conditions. Furthermore, the interaction between different dyes and membrane surfaces was systematically elucidated, especially when high salinity (i.e., NaCl) was present in dye solutions. Finally, fractionation of dye/NaCl binary mixtures through the overall diafiltration process (including a pre-concentration step and a diafiltration step) was demonstrated by the commercial loose NF membrane with model validation.

2. Experimental section

2.1. Chemicals and membrane

Two reactive dyes (reactive blue 2 (RB 2) and reactive orange 16 (RO 16)) and four cationic dyes (neutral red (NR), methylene blue (MB), malachite green oxalate (MGO), and rhodanile blue (RB)) from Sigma Aldrich (Belgium) were used as model dyes. The molecular structures of these model dyes are shown in Fig. 1. NaCl (analytical grade, 99.5% purity) was also supplied by Sigma Aldrich. All the chemicals were used as received. Ultrapure water (electrical resistance with 18.2 MΩ·cm) was used throughout the experiments.

A commercial thin film composite loose NF membrane (Sepro NF 2A, Ultura, USA) was employed in this study. This NF membrane has semi-aromatic polyamide chemistry (poly-piperazineamide) with a highly hydrophilic loose surface, high pure water permeability, and low NaCl rejection [19] (Table 1).

2.2. Nanofiltration tests

Filtration performance of the NF membrane for dye solutions was investigated with a cross-flow permeation cell with an effective area of 22.9 cm^2 [4]. Prior to the filtration experiments, the NF membrane was

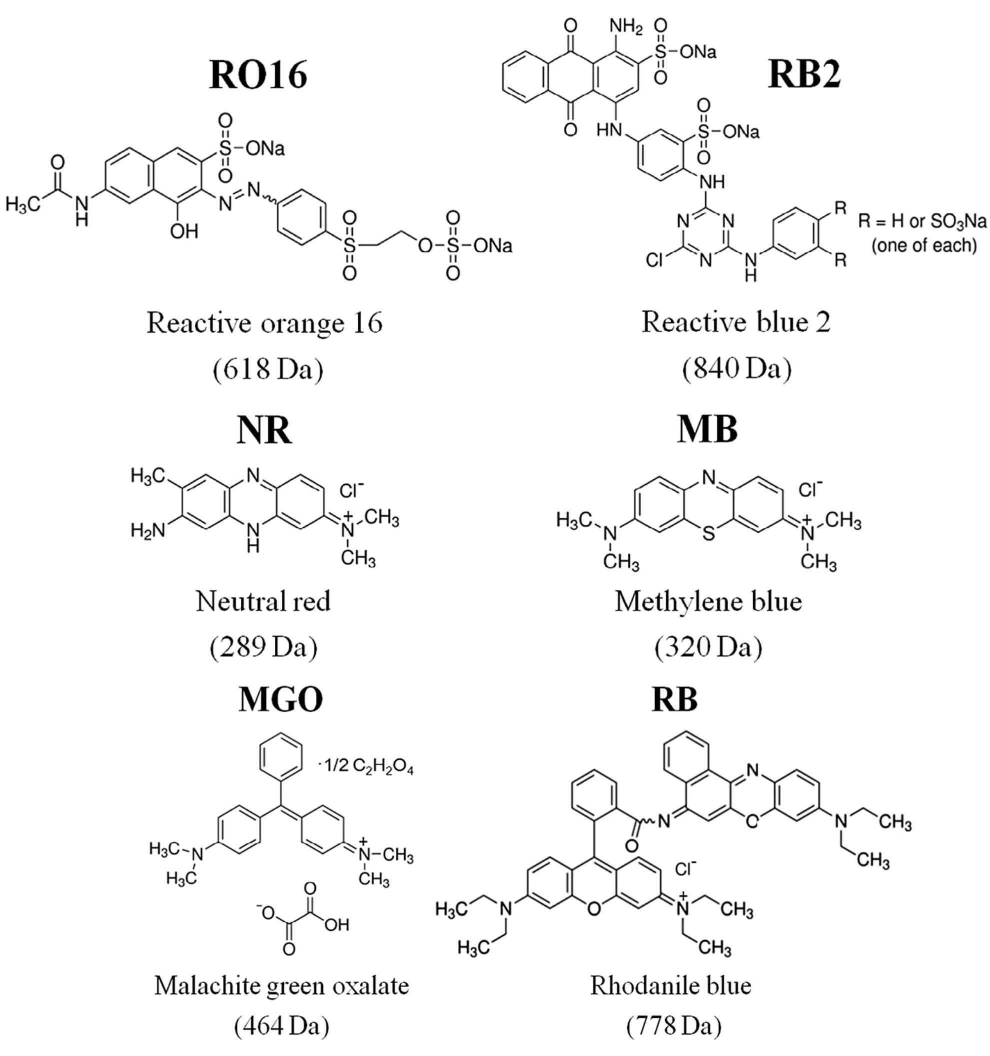

Fig. 1. Molecular structures of the model dyes tested in this study.

Table 1
Characteristics of the loose NF membrane used in this study [19].

Membrane	Contact angle (°)	MWCO (Da)	PWP at 25 °C ($L\,m^{-2}\,h^{-1}\cdot bar^{-1}$)[a]	NaCl rejection (%)[b]	Zeta potential at pH7 (mV)
Sepro NF 2A	21.7 ± 1.4	490	10.2 ± 0.6	21.8	−55

[a] PWP denotes the pure water permeability.
[b] Rejection of 1 $g\,L^{-1}$ NaCl solution at 6 bar and 25 °C, obtained experimentally in this work.

pre-compacted with pure water at 10 bar and 25 ± 1 °C for 2 h to achieve a steady flux. Initial filtration experiments were conducted with a single dye solution at different operating pressures and dye concentrations. Subsequently, filtration of multi-component solutions (i.e., dye/NaCl mixtures) was performed at 6 bar and cross-flow rate of 60 $L\,h^{-1}$.

Afterwards, an integrated process, including a pre-concentration step and a diafiltration step, in a batch mode was designed for dye desalination and purification from dye/salt mixtures (Fig. 2). Initially, 1000 mL dye solution (i.e., 2 $g\,L^{-1}$ dye and ca. 40 $g\,L^{-1}$ NaCl) as the feed was concentrated by a factor of 5.0 to reduce the water consumption in the diafiltration stage. Subsequently, diafiltration was performed while adding pure water to the feed at the same rate as the permeate to keep the feed volume constant. Both pre-concentration and diafiltration stages were performed at 6 bar and 25 ± 1 °C.

The permeation flux (J) and rejection coefficient (R) of the loose NF membrane were calculated by Eqs. (1) and (2), respectively:

$$J = \frac{V}{A\cdot t} \tag{1}$$

$$R(\%) = \frac{C_f - C_p}{C_f} \times 100 \tag{2}$$

where V is the water volume collected during time interval t, A denotes the effective membrane area for water permeation, and C_f and C_p are the solute concentration of the feed and permeate, respectively.

2.3. Membrane flux calculation

Generally, membrane fouling and concentration polarization inevitably occur during the filtration of organic matters and salt mixtures, e.g. dye/salt mixtures [20]. Therefore, the permeate flux (J_w) can be described by the resistance-in-series model:

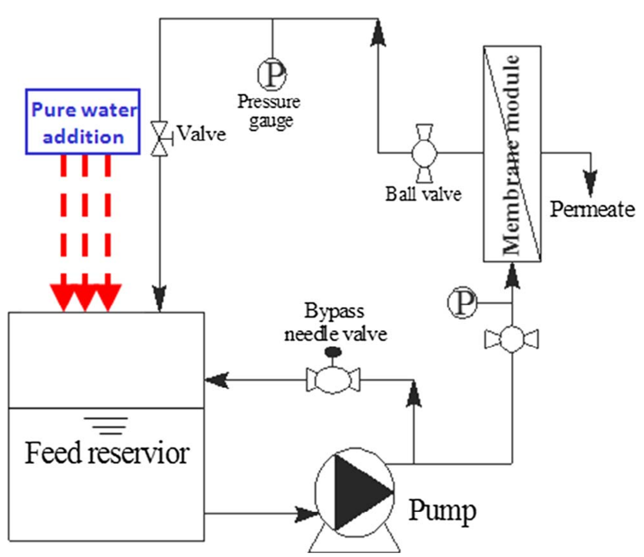

Fig. 2. Schematic of the over diafiltration process by NF membrane. (Pre-concentration stage allows for no water addition to reduce of feed volume; diafiltration stage requires the addition of pure water to remove the salt from the feed).

$$J_W = \frac{\Delta P - \Delta \pi}{\mu (R_m + R_f + R_{cp})} \tag{3}$$

where ΔP represents the trans-membrane pressure, $\Delta\pi$ denotes the osmotic pressure difference between bulk and permeate solution, μ represents the viscosity of solution, R_m denotes the intrinsic membrane resistance, R_f is the hydraulic resistance caused by fouling and R_{cp} represents the resistance induced by concentration polarization of inorganic salts.

For a multi-component solution, the osmotic pressure difference ($\Delta\pi$) between the two sides of the loose NF membrane can be calculated by superimposing the contribution from each individual component (i) in the solution [21]:

$$\Delta\pi = \sum_{i=1}^{i=n} \Delta\pi_i = \Delta\pi_1 + \Delta\pi_2 + \Delta\pi_3 + \cdots + \Delta\pi_n \tag{4}$$

For a dilute solution, the osmotic pressure can be estimated by the Van't Hoff Equation:

$$\pi_i = C_i R_g T \tag{5}$$

where C_i is the molarity of component (i), R_g is the universal gas constant, and T is the thermodynamic (absolute) temperature.

To calculate the theoretical membrane flux in a dye/salt mixture from Eq. (3), the intrisnic membrane resistance (R_m) was determined from the flux of pure water, the hydraulic resistance caused by fouling (R_f) was calculated from independent filtration test using single dye solution, and the resistance from the concentration polarization of NaCl (R_{cp}) was determined by independent filtration of NaCl solutions.

2.4. Dye purification simulation

The overall process for dye purification in the pigment industry involves a pre-concentration step and a diafiltration step. To quantify the concentration of solutes (i.e., dye and salt), a simulation of the overall diafiltration process for the fractionation of dye/salt mixtures was conducted, as described by Wang et al. and Kim et al. [22,23] (see the derivation in Supplementary Information). The concentration (C_f^t) of the dye and salt in the pre-concentration step can be expressed by:

$$C_f^t = C_f^0 \cdot \eta_1^{R_f} \tag{6}$$

where C_f^0 denotes the initial concentration of the dye or salt in the pre-concentration step, η_1 is the concentration factor of the feed solution, defined as the ratio of the initial feed volume (V_f^0) to the ultimate volume (V_f^t) during the pre-concentration step, and R_f presents the observed rejection coefficient to solutes in the pre-concentration step.

Furthermore, the concentration (C_d^t) of the dye and salt in the

Table 2
Filtration performance of Sepro NF 2A membrane for reactive or cationic dyes of 0.05 $g\,L^{-1}$ at 2 bar.

Dye	Permeate flux ($L\cdot m^{-2}\cdot h^{-1}$)	Rejection (%)
NR (289 Da)	19.5	88.7
MB (320 Da)	20.7	85.0
MGO (464 Da)	19.9	96.4
RO 16 (618 Da)	20.1	99.7
RB (778 Da)	20.9	98.6
RB 2 (840 Da)	20.1	99.9

Table 3
Separation performance of various commercial and lab-made NF membranes for dye desalination.

Membranes (MWCO)	Permeability ($L\,m^{-2}h^{-1}\cdot bar^{-1}$)	Type of dyes (MW)	Dye rejection	NaCl rejection (Salt content)	α[a]	Ref.
UTC-60 (~150 Da)	10.0	RO 16 (618 Da)	97.9%	30.1% ($0.58\,g\,L^{-1}$)	33.3	[10]
DS5 DK (150–300)	6.6	Reactive black 5 (992 Da)	99.5%	47.5% ($0.58\,g\,L^{-1}$)	105.0	[7,24]
Polyethylenimine based membrane (511 Da)	9.5	Cationic gold yellow X-GL (434 Da)	96.4%	50.0% ($1\,g\,L^{-1}$)	13.9	[25]
Cellulose acetate NF membrane (520 Da)	3.9	Reactive black 5 (992 Da)	99.1%	58.2% ($2\,g\,L^{-1}$)	46.4	[26]
NF hollow fiber membrane (520 Da)	11.9	Cationic red X-GTL (502 Da)	99.7%	39.5% ($1\,g\cdot L^{-1}$)	201.7	[27]
BHAC-PIP composite membrane (570 Da)	8.5	Methyl blue (800 Da)	98.9%	57.8% ($0.5\,g\,L^{-1}$)	38.4	[28]
HNTs-poly(NASS)/PES membrane (784 Da)	10.8	Reactive black 5 (992 Da)	85.5%	6.9% ($1\,g\,L^{-1}$)	6.4	[29]
Sepro NF 2A (490 Da)	10.2	RB (778 Da) RO 16 (618 Da)	98.6% 99.7%	17.2% ($2\,g\,L^{-1}$)	59.1 276.0	This work

[a] α denotes the selectivity of dye over Cl^-, calculated by $\alpha = (1 - R_{NaCl})/(1 - R_{dye})$.

diafiltration step can be described by:

$$C_d^t = C_d^0\cdot\exp[-\eta_2\cdot(1-R_d)] \tag{7}$$

where C_d^0 denotes the initial concentration of the solute in the diafiltration step, η_2 is the number of diavolume, defined as the ratio of the total collected filtrate volume (V_w) to the constant feed (V_d^0) during the diafiltration step, and R_d presents the observed rejection coefficient to solutes in the diafiltration step.

2.5. Analytical methods

The concentrations of reactive and cationic dyes were determined by a Shimadzu UV-1601 double beam spectrophotometer (Japan) based on the Lambert-Beer's Law. The concentration of NaCl in the dye/salt mixture solutions was analyzed by ion chromatography (Dionex ICS-2000 Ion Chromatography System, USA) by determining the Cl^- concentration. It is worth noting that before the measurement of Cl^- ions in the dye/salt mixed solution, clean granular activated carbon was applied for complete adsorption of dyes to avoid the contamination of the analytic column/assay.

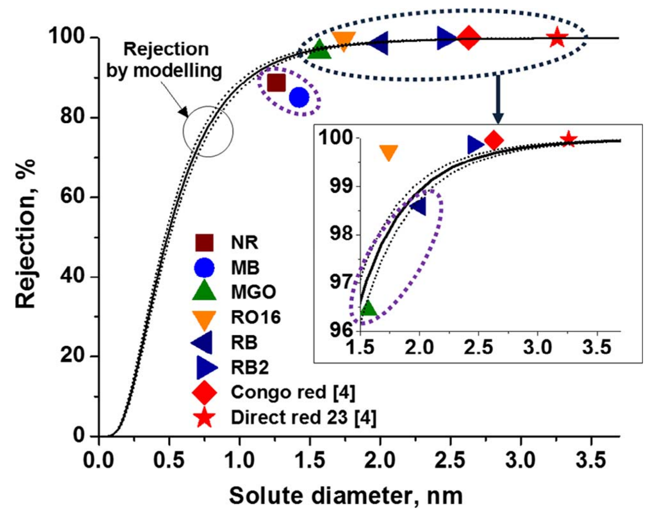

Fig. 3. Relationship between the rejection of Sepro NF 2A membrane and diameters of various dyes (Data of Congo red and direct red 23 are derived from Ref. [4]).

3. Results and discussion

3.1. Filtration of dye solutions

3.1.1. Retention mechanism for different dyes

To study the potential of the loose NF membrane in the filtration of reactive dyes and cationic dyes with different molecular weights, the dye rejection and filtrate flux of the loose NF membrane with different dye solutions of $0.05\,g\,L^{-1}$ at 2 bar and 25 ± 1 °C were measured (Table 2).

As indicated in Table 2, Sepro NF 2A membrane had a high rejections (> 99%) for aqueous reactive dye solutions (i.e., RO 16 and RB 2). However, lower rejection for cationic dyes can be clearly observed, mainly due to their lower molecular weights. Compared with other reported NF membranes for dye/salt separation (Table 3), Sepro NF 2A membrane showed a comparable permeability and selectivity, suggesting a strong potential for minimizing dye loss, particularly when the diafiltration process is employed for dye desalination and purification.

Generally, the transport mechanism of dye molecules through NF membranes involves size exclusion, electrostatic repulsion and adsorptive interaction [4,30,31]. Van der Bruggen et al. demonstrated that the size exclusion effect dominates the retention of reactive dyes in NF [10]. To elucidate the filtration mechanism of this NF membrane for dye retention, the relationship between retention coefficient of various dyes and their diameter parameter (i.e., the length of various dyes shown in Supplementary Fig. S1) was determined (Fig. 3).

In Fig. 3, the measured rejections to reactive dyes (i.e., RB 2 and RO 16) of the loose NF membrane are higher than the theoretical values derived from the log-normal model [19] (Supplementary Fig. S2), presenting a higher dye retention than the theoretical value. This is likely attributed to the aggregation of dye molecules [32], which increases their effective size and thus rejection of the loose NF membrane. Similar dye aggregation phenomena have been reported for direct dyes (i.e., Congo red and direct red 23) – dye molecules clustering together via hydrophobic interactions between their aromatic rings [20]. Furthermore, electrostatic repulsion can be substantially boosted for the retention of reactive dye clusters with multiple negative charges caused by dye aggregation.

In constrast, we observed an opposite trend for the cationic dyes (NR, MB, MGO and RB, as marked in dash purple[1] circle in Fig. 3), with

[1] For interpretation of color in Fig. 3, the reader is referred to the web version of this article.

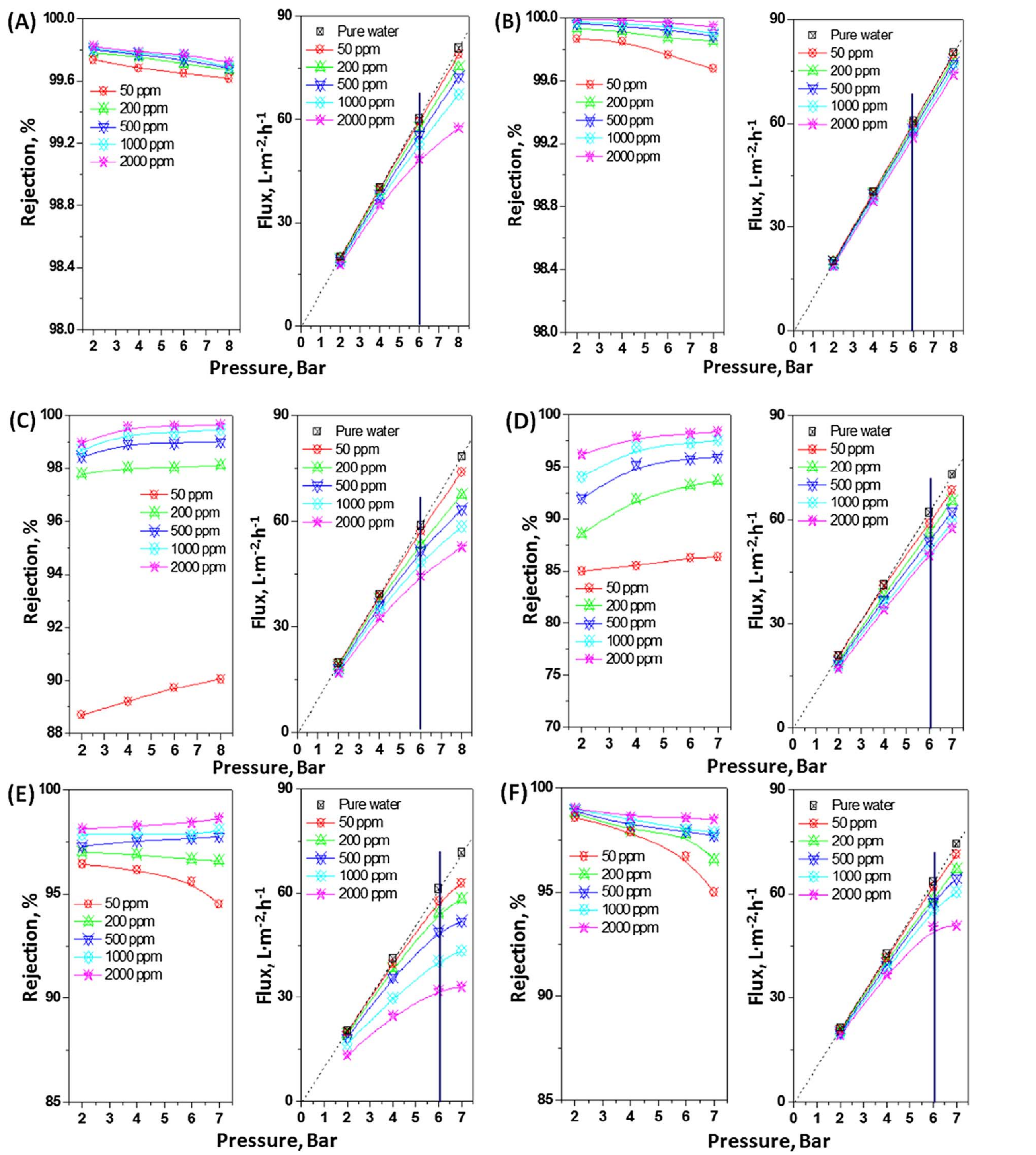

Fig. 4. Solute rejection and water flux of Sepro NF 2A membrane with various dyes. (A): RO 16; (B): RB 2; (C): NR; (D): MB; (E): MGO; (F): RB.

experimental rejections generally lower than the predicted rejections based on size exclusion alone. This trend can be explained by the electrostatic attraction interaction between the cationic dyes and the negatively charged membrane surface (see Supplementary Fig. S3), which promotes the sorption of cationic dyes onto Sepro NF 2A membrane and facilitates their transport through the membrane.

3.1.2. Influence of operational pressure and dye concentration on dye rejection

To further explore the applicability of the loose NF membrane for dye recovery and concentration, the effect of operational pressure and dye concentration on membrane performance was investigated (Fig. 4).

As seen in Fig. 4, increasing dye concentration improved the dye rejection due to the increase in effective size of the dye clusters originated from more favorable dye aggregation at higher dye concentrations. This is consistent with literature reports for other organic molecules [33]. Similar to the case of anionic dyes (e.g., direct dyes and reactive dyes), intermolecular interaction between the cationic dyes also plays a significant role in filtration performance of the NF membrane. For instance, Rabinowitch and Epstein [34] investigated the structure-reactivity correlations of methylene blue (MB), observing that the polymerization of methylene blue ($2MB^+ \rightleftharpoons (MB)_2^{2+}$ equilibrium) takes place at high dye concentrations through the association of the dyestuff cations, which can expand the size of methylene blue dimers for its enhanced rejection. This noticeably demonstrates that regardless of charge of dyes, dye aggregation can be a crucial factor in NF performance, which should be carefully taken into consideration. At the meantime, the water flux of the NF membrane was reduced with increasing dye concentration, likely caused by increased osmotic pressure of the dyes at the higher concentration, in addition to membrane fouling.

Furthermore, higher water flux was obtained at increasing the applied operating pressure. However, this increase appeared to be highly non-linear probably as a result of severe concentration polarization and/or membrane fouling (see the cake layer in Supplementary Fig. S4) [35]. This indicates that increasing operating pressure above the threshold value fails to enhance the membrane permeability. As shown in Fig. 4, the threshold pressure of Sepro NF 2A during the filtration of dye solutions lied at 6 bar in the current case. Simultaneously, we observed a decreased dye rejection at higher pressures for a number of cases, an effect that was particularly pronounced at lower dye concentration. The decrease in rejections is somewhat counter-intuitive, as one would expect enhanced rejection at higher pressures as a result of enhanced dilution effect – a great passage of water flux helps to reduce the effective solute concentration in the permeate water. This apparent contradiction in rejection behaviors, together with the non-linear flux response, suggests that concentration polarization played an important role in the current study. Concentration polarization also explains why the greatest reduction in dye rejection occurred for Sepro NF 2A membrane with 0.05 g L^{-1} dye concentration, with a combination that led to higher water flux.

3.1.3. Effect of salt addition on filtration of dye solutions

In order to elucidate the effect of salt present in the dye solutions on the membrane performance, the filtration behavior of Sepro NF 2A membrane in dye/salt mixtures with different salt concentrations at the applied pressure of 6 bar was investigated (Fig. 5).

Fig. 5 shows that the rejection of dyes for the loose NF membrane decreased with the addition of salt in the dye/salt mixtures. Remarkably, the presence of NaCl had a more significant impact on the retention of cationic dyes. For instance, the rejection of MGO for this NF membrane dropped sharply from 98.5% to 96.5% when the NaCl concentration increased to 60 g L^{-1}. On one hand, the membrane swelling induced by elevated NaCl concentration due to the integrated contribution of repulsion forces between counter-ions inside the pore walls and the decrease in thickness of the hydration layer on the pore walls through the salting-out effect, resulting in a slight enlargement in pore size of NF membrane surface, could boost the transport of the cationic dyes with smaller molecular size through Sepro NF 2A membrane [36–41]. On the other hand, the background electrolytes (i.e., NaCl) in the dye solution can substantially shield the electrostatic double layer interaction [22,42], which diminishes the dielectric effect of the NF membrane for reducing the dye rejection. Furthermore, due to the decreasing flux caused by the osmotic pressure, the transport of (cationic) dyes via solution-diffusion is increasingly comparable to that originated from reducing convection of the permeation flow through the NF membrane, which can partially lower the rejection of dyes. However, these (reactive and cationic) dyes have no obvious impact on the NaCl rejection of Sepro NF 2A membrane which shows the similarly low salt rejection in dye/salt mixtures, compared to that in pure NaCl solutions (see Supplementary Fig. S5).

Fig. 5 also indicates that the flux of the loose NF membrane in all the dye/salt binary mixtures dropped with the increasing salt concentrations. Noticeably, the measured flux for Sepro NF 2A membrane is significantly lower than the theoretical membrane flux which is calculated by Eq. (3). This is due to the cake-enhanced concentration polarization, resulting in flux decline, which is consistent with the case of direct dyes [20].

3.2. Simulation for pre-concentration and diafiltration

On the basis of the retention results for dye/NaCl mixtures in Fig. 5, a simulation on diafiltration by the NF membrane was performed as a guideline for its practical application in purification of dyes (Fig. 6). In this case, the integrated diafiltration process, including pre-concentration and diafiltraion step, was performed in a batch mode.

Fig. 6(A) shows the concentration ratio of dye or salt (C_f^t/C_f^0) as a function of the concentration factor (η_1) in the pre-concentration step

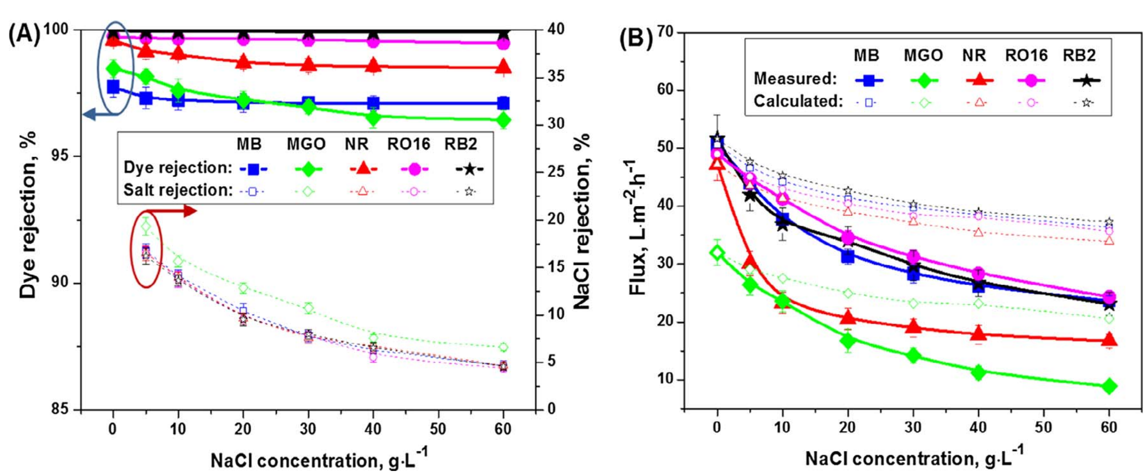

Fig. 5. Filtration performance of Sepro NF 2A membrane after salt addition with different concentrations. (A): Solute rejection; (B): membrane flux.

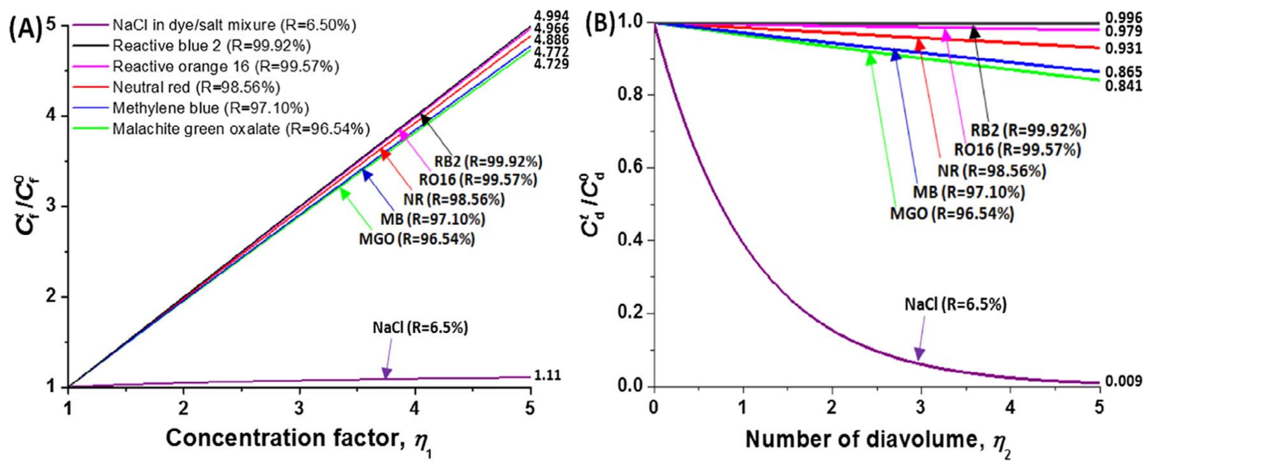

Fig. 6. Simulation of dye or salt concentration as a function of the concentration factor (η_1) at the pre-concentration step (A) and number of diavolume (η_2) at the diafiltration step (B) in the overall diafiltration process by Sepro NF 2A membrane in batch mode.

for dye/salt mixtures, derived from Eq. (6). In this case, the concentration of dye and salt was fixed at $2\,g\,L^{-1}$ and $40\,g\,L^{-1}$, respectively. The rejection to NaCl of the loose NF membrane in different dye solutions was considered constant. As indicated in Fig. 6(A), C_f^t/C_f^0 increases rapidly with the evolution of η_1 for the case of dyes with high observed rejection and vice versa for NaCl, indicating a promising fractionation performance of the loose NF membrane.

Following the pre-concentration step, the subsequent diafiltration step was conducted to remove the NaCl impurity for desalination and purification of dye solution. Fig. 6(B) shows the concentration ratio of dye or salt (C_d^t/C_d^0) as a function of the number of diavolume (η_2) in diafiltration step for dye desalination, derived from Eq. (7). The concentration of solute decreases with the volume factor for added pure water in diafiltration (Fig. 6B). Specifically, the concentration of NaCl with low observed rejection decays quickly with the addition of pure water, and slowly for the case of dyes with high observed rejection.

Through the simulation for the overall diafiltration process, a dye with high rejection can be effectively retained and NaCl with low rejection can be sufficiently washed out from the dye/NaCl mixture as demonstrated in Fig. 7. Through integration of pre-concentration with concentration factor of 5.0 and diafiltration with 5.0 diavolumes, 0.2% NaCl was obtained in the feed solution, indicating a sufficient desalination and purification of dyes. Specifically, the reactive dyes (i.e., RB 2 and RO 16) have a >97.2% yield after the overall diafiltration process.

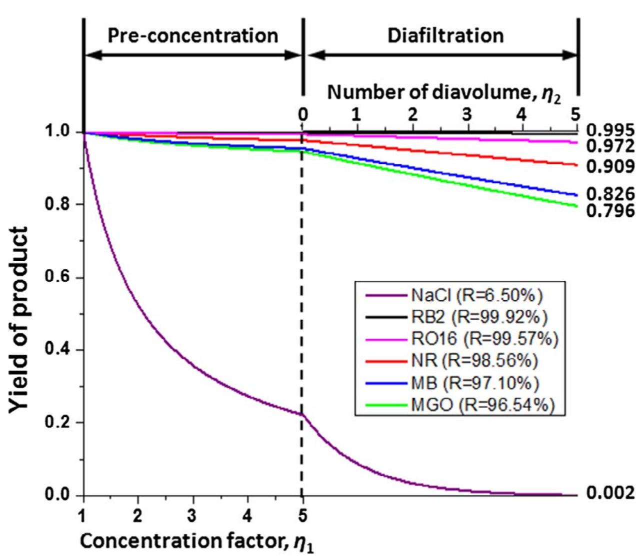

Fig. 7. Simulation of the yield for dye and salt during the overall diafiltration process by Sepro NF 2A membrane.

3.1.5. Loose nanofiltration-diafiltration of dye/salt mixtures

In order to effectively fractionate the dye/salt mixture to enhance the purity of dye products for digital printing, the overall diafiltration, including pre-concentration step and diafiltration by NF for different dyes (RB 2, RO 16 and MB) was designed (Fig. 8 and Supplementary Fig. S6).

As shown in Fig. 8(A) and (B), the concentration of reactive dyes (i.e., RB 2 and RO 16) in the pre-concentration step performed by the loose NF membrane increases sharply from $2.0\,g\,L^{-1}$ to ca. $10.1\,g\,L^{-1}$ with the concentration factor of 5.0. Meanwhile, the concentration of NaCl in the feed slightly increases by a factor of 1.12, equivalent to ca. 77.7% salt removal. Subsequently, the diafiltration procedure can effectively remove NaCl from the reactive dye solutions. With 5.0 diavolumes, the concentration of NaCl in the dye solution dropped to $1.3\,g\,L^{-1}$, equivalent to an overall salt removal of 99.3% in the integrated process, due to the extremely low salt rejection (ca. 6.3% to 25.5%). Simultaneously, almost complete rejection (>99.5%) for reactive dyes results in only ca. 2.0% dye loss (see Supplementary Fig. S6(A) and (B)). During the diafiltration of MB as model cationic dye in Fig. 8(C), the loose NF membrane exhibits an acceptably high rejection (97.2%) for MB and 99.4% salt removal in the MB/NaCl mixture, establishing an effective approach for the fractionation of dye/NaCl mixture. Compared to reactive dyes, a lower rejection for MB results in a greater dye loss (15.9% for MB) by Sepro NF 2A membrane in the permeate after diafiltration with 5.0 diavolumes (see Supplementary Fig. S6(C)).

4. Conclusions

In this study, the loose commercial 'Sepro NF 2A' nanofiltration membrane with MWCO of 490 Da was investigated for fractionation of NaCl from two reactive and four cationic ink-jet dyes. Acceptably, this NF membrane can sufficiently retain the dyes, yielding a dye rejection higher than 97.7%. The electrostatic attraction had a negative impact on the dye retention of the NF membrane with negative charges during

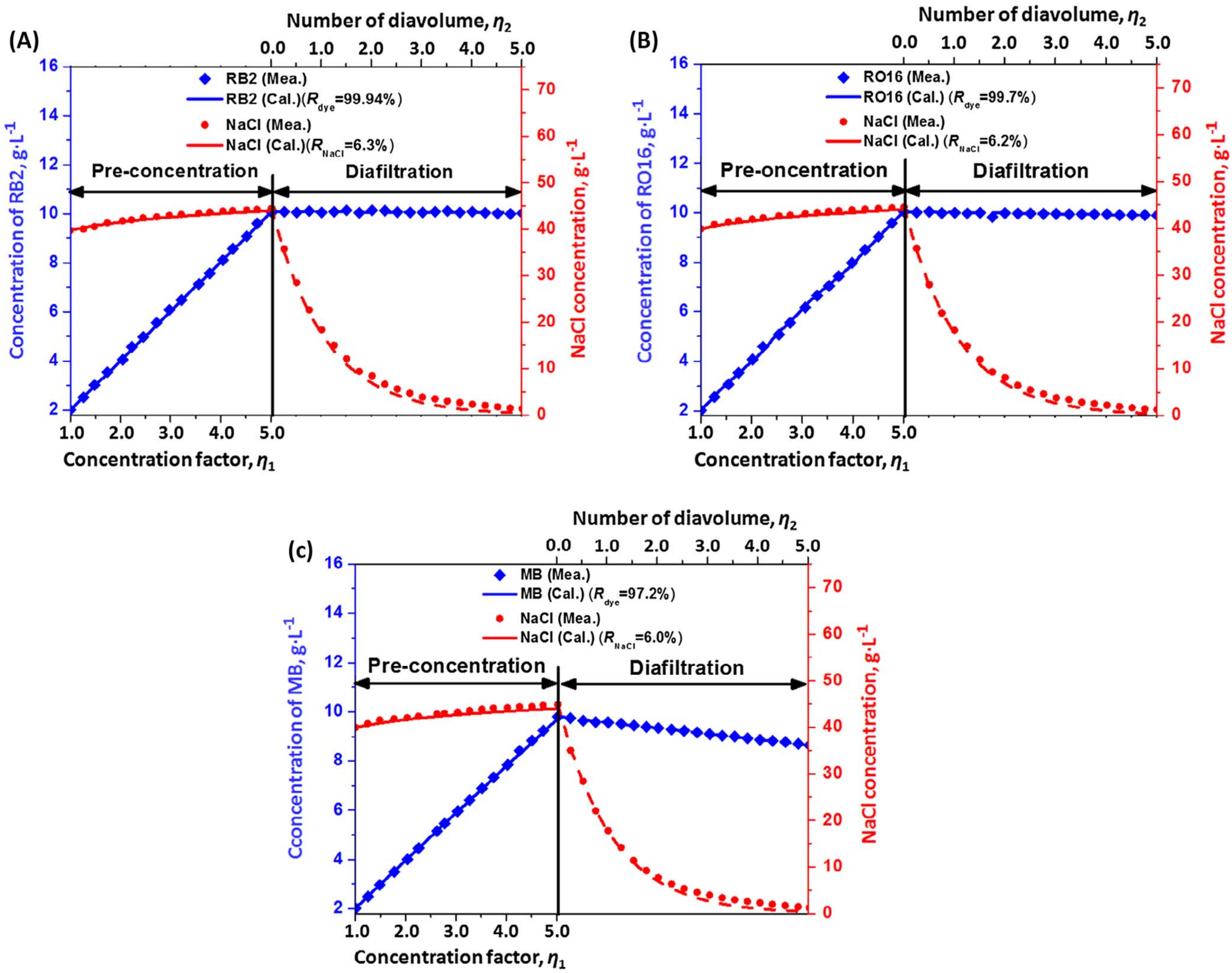

Fig. 8. Overall diafiltration process for different dye solutions by Sepro NF 2A membrane. (A): RB 2; (B): RO 16; (C): MB.

the filtration of cationic dyes. However, the high salinity of the dye/NaCl mixtures would not substantially compromise the dye rejection of the loose NF membrane, indicating its strong potential for advanced purification of diverse dye/NaCl mixtures in industrial applications.

For two reactive dyes (reactive blue 2 and reactive orange 16) with rejection higher than 99.7%, this integrated NF-diafiltration process, including pre-concentration and diafiltration with 5 diavolumes, yields ca. 99.3% salt removal with only 2.0% dye loss. Simultaneously, the loose NF membrane experienced 15.9% of dye loss due to its moderate rejection to methylene blue (97.2%) but had a similar salt removal (99.4%) at the same operational condition.

Acknowledgment

W. Ye and J. Lin would like to thank the funding support from the National Natural Science Foundation of China (Grants Nos. 21706035 and 21707018), the Natural Science Foundation of Fujian Province (Grant No. 2017J01413), the Fujian Agriculture and Forestry University Program for Distinguished Young Scholar (Grant No. xjq201704) and Fuzhou University (Grants Nos. XRC-1622 and 2017T017) for this work. Ultura, USA, is greatly thanked for providing the nanofiltration membrane samples. The authors also thank Nicole J. Bernstein from the Pennsylvania State University (USA) for the structure simulation of dye molecules.

Appendix A. Supplementary material

Supplementary data associated with this article can be found, in the online version, at http://dx.doi.org/10.1016/j.seppur.2017.12.045.

References

[1] C. Xue, Q. Chen, Y. Liu, Y. Yang, D. Xu, L. Xue, W. Zhang, Acid blue 9 desalting using electrodialysis, J. Membr. Sci. 493 (2015) 28–36.
[2] Y. He, G. Li, H. Wang, J. Zhao, H. Su, Q. Huang, Effect of operating conditions on separation performance of reactive dye solution with membrane process, J. Membr. Sci. 321 (2008) 183–189.
[3] W. Ding, H. Zhuo, M. Bao, Y. Li, J. Lu, Fabrication of organic-inorganic nanofiltration membrane using ordered stacking SiO_2 thin film as rejection layer assisted with layer-by-layer method, Chem. Eng. J. 330 (2017) 337–344.
[4] J. Lin, W. Ye, H. Zeng, H. Yang, J. Shen, S. Darvishmanesh, P. Luis, A. Sotto, B. Van der Bruggen, Fractionation of direct dyes and salts in aqueous solution using loose nanofiltration membranes, J. Membr. Sci. 477 (2015) 183–193.
[5] J. Zhu, M. Tian, Y. Zhang, H. Zhang, J. Liu, Fabrication of a novel loose nanofiltration membrane by facile blending with Chitosan-Montmorillonite nanosheets for dyes purification, Chem. Eng. J. 265 (2015) 184–193.
[6] M. Mondal, S. De, Treatment of textile plant effluent by hollow fiber nanofiltration membrane and multi-component steady state modeling, Chem. Eng. J. 285 (2016) 304–318.
[7] I. Koyuncu, Reactive dye removal in dye/salt mixtures by nanofiltration membranes containing vinylsulphone dyes: effects of feed concentration and cross flow velocity, Desalination 143 (2002) 243–253.
[8] C. Tang, V. Chen, Nanofiltration of textile wastewater for water reuse, Desalination 143 (2002) 11–20.
[9] Z. Badani, C. Cabassud, H. Ait-Amar, Membrane separation process for the

treatment and reuse of bath dye effluents, Desalin. Water Treat. 9 (2009) 105–111.
[10] B. Van der Bruggen, B. Daems, D. Wilms, C. Vandecasteele, Mechanisms of retention and flux decline for the nanofiltration of dye baths from the textile industry, Sep. Purif. Technol. 22–23 (2001) 519–528.
[11] I. Koyuncu, D. Topacik, M.R. Wiesner, Factors influencing flux decline during nanofiltration of solutions containing dyes and salts, Water Res. 38 (2004) 432–440.
[12] J. Zhu, A. Uliana, J. Wang, S. Yuan, J. Li, M. Tian, K. Simoens, A. Volodin, J. Lin, K. Bernaerts, Y. Zhang, B. Van der Bruggen, Elevated salt transport of antimicrobial loose nanofiltration membranes enabled by copper nanoparticles via fast bioinspired deposition, J. Mater. Chem. A 4 (2016) 13211–13222.
[13] F. Liu, B. Ma, D. Zhou, L. Zhu, Y. Fu, L. Xue, Positively charged loose nanofiltration membrane grafted by diallyl dimethyl ammonium chloride (DADMAC) via UV for salt and dye removal, React. Funct. Polym. 86 (2015) 191–198.
[14] P. Chen, X. Ma, Z. Zhong, F. Zhang, W. Xing, Y. Fan, Performance of ceramic nanofiltration membrane for desalination of dye solutions containing NaCl and Na_2SO_4, Desalination 404 (2017) 102–111.
[15] T. Chidambaram, Y. Oren, M. Noel, Fouling of nanofiltration membranes by dyes during brine recovery from textile dye bath wastewater, Chem. Eng. J. 262 (2015) 156–168.
[16] Y.K. Ong, F.Y. Li, S. Sun, B. Zhao, C. Liang, T. Chung, Nanofiltration hollow fiber membranes for textile wastewater treatment: lab-scale and pilot-scale studies, Chem. Eng. Sci. 114 (2014) 51–57.
[17] S.P. Sun, T.A. Hatton, S.Y. Chan, T. Chung, Novel thin-film composite nanofiltration hollow fiber membranes with double repulsion for effective removal of emerging organic matters from water, J. Membr. Sci. 401–402 (2012) 152–162.
[18] Y.C. Xu, Z.X. Wang, X.Q. Cheng, Y.C. Xiao, L. Shao, Positively charged nanofiltration membranes via economically mussel-substance-simulated co-deposition for textile wastewater treatment, Chem. Eng. J. 303 (2016) 555–564.
[19] J. Lin, C.Y. Tang, C. Huang, Y.P. Tang, W. Ye, J. Li, J. Shen, R. Van den Broeck, J. Van Impe, A. Volodin, C. Van Haesendonck, A. Sotto, P. Luis, B. Van der Bruggen, A comprehensive physico-chemical characterization of superhydrophilic loose nanofiltration membranes, J. Membr. Sci. 501 (2016) 1–14.
[20] J. Lin, C.Y. Tang, W. Ye, S. Sun, S.H. Hamdan, A. Volodin, C.V. Haesendonck, A. Sotto, P. Luis, B. Van der Bruggen, Unraveling flux behavior of superhydrophilic loose nanofiltration membranes during textile wastewater treatment, J. Membr. Sci. 493 (2015) 690–702.
[21] K.M. Pastagia, S. Chakraborty, S. DasGupta, J.K. Basu, S. De, Prediction of permeate flux and concentration of two-component dye mixture in batch nanofiltration, J. Membr. Sci. 218 (2003) 195–210.
[22] X. Wang, C. Zhang, P. Ouyang, The possibility of separating saccharides from a NaCl solution by using nanofiltration in diafiltration mode, J. Membr. Sci. 204 (2002) 271–281.
[23] J.F. Kim, A.M. Freitas Da Silva, I.B. Valtcheva, A.G. Livingston, When the membrane is not enough: a simplified membrane cascade using Organic Solvent Nanofiltration (OSN), Sep. Purif. Technol. 116 (2013) 277–286.
[24] A.W. Mohammad, R.K. Basha, C.P. Leo, Nanofiltration of glucose solution containing salts: Effects of membrane characteristics, organic component and salts on retention, J. Food Eng. 97 (2010) 510–518.
[25] X. Wei, S. Wang, Y. Shi, H. Xiang, J. Chen, Application of positively charged composite hollow-fiber nanofiltration membranes for dye purification, Ind. Eng. Chem. Res. 53 (2014) 14036–14045.
[26] S. Yu, M. Liu, M. Ma, M. Qi, Z. Lü, C. Gao, Impacts of membrane properties on reactive dye removal from dye/salt mixtures by asymmetric cellulose acetate and composite polyamide nanofiltration membranes, J. Membr. Sci. 350 (2010) 83–91.
[27] X. Wei, X. Kong, C. Sun, J. Chen, Characterization and application of a thin-film composite nanofiltration hollow fiber membrane for dye desalination and concentration, Chem. Eng. J. 223 (2013) 172–182.
[28] T. Wang, Y. Yang, J. Zheng, Q. Zhang, S. Zhang, A novel highly permeable positively charged nanofiltration membrane based on a nanoporous hyper-crosslinked polyamide barrier layer, J. Membr. Sci. 448 (2013) 180–189.
[29] J. Zhu, N. Guo, Y. Zhang, L. Yu, J. Liu, Preparation and characterization of negatively charged PES nanofiltration membrane by blending with halloysite nanotubes grafted with poly (sodium 4-styrenesulfonate) via surface-initiated ATRP, J. Membr. Sci. 465 (2014) 91–99.
[30] A.C. Gomes, I.C. Gonçalves, M.N.D. Pinho, The role of adsorption on nanofiltration of azo dyes, J. Membr. Sci. 255 (2005) 157–165.
[31] L.D. Nghiem, A.I. Schäfer, T.D. Waite, Adsorptive interactions between membranes and trace contaminants, Desalination 147 (2002) 269–274.
[32] P. Skrabal, F. Bangerter, K. Hamada, T. Iijima, Entropy contribution to an azo dye aggregation in aqueous solution, Dyes Pigm. 8 (1987) 371–374.
[33] J.M. Arsuaga, M.J. López-Muñoz, J. Aguado, A. Sotto, Temperature, pH and concentration effects on retention and transport of organic pollutants across thin-film composite nanofiltration membranes, Desalination 221 (2008) 253–258.
[34] E. Rabinowitch, L.F. Epstein, Polymerization of dyestuffs in solution. Thionine and methylene blue, J. Am. Chem. Soc. 63 (1941) 69–78.
[35] J. Luo, L. Ding, Y. Wan, M.Y. Jaffrin, Threshold flux for shear-enhanced nanofiltration: experimental observation in dairy wastewater treatment, J. Membr. Sci. 409–410 (2012) 276–284.
[36] M. Nilsson, G. Trägårdh, K. Östergren, The influence of pH, salt and temperature on nanofiltration performance, J. Membr. Sci. 312 (2008) 97–106.
[37] V. Freger, T.C. Arnot, J.A. Howell, Separation of concentrated organic/inorganic salt mixtures by nanofiltration, J. Membr. Sci. 178 (2000) 185–193.
[38] J. Luo, S. Wei, Y. Su, X. Chen, Y. Wan, Desalination and recovery of iminodiacetic acid (IDA) from its sodium chloride mixtures by nanofiltration, J. Membr. Sci. 342 (2009) 35–41.
[39] J. Luo, Y. Wan, Effect of highly concentrated salt on retention of organic solutes by nanofiltration polymeric membranes, J. Membr. Sci. 372 (2011) 145–153.
[40] J. Luo, L. Ding, X. Chen, Y. Wan, Desalination of soy sauce by nanofiltration, Sep. Purif. Technol. 66 (2009) 429–437.
[41] J. Luo, Y. Wan, Effects of pH and salt on nanofiltration – A critical review, J. Membr. Sci. 438 (2013) 18–28.
[42] J. Qin, X. Dai, Y. Zhou, L. Zhang, H. Chen, C. Gao, Desalting and recovering naphthalenesulfonic acid from wastewater with concentrated bivalent salt by nanofiltration process, J. Membr. Sci. 468 (2014) 242–249.